

Modeling curvelet domain inter-band image statistics with application to spatially adaptive image denoising

L. Tessens, A. Pižurica and W. Philips
TELIN, Ghent University
St-Pietersnieuwstraat 41
B-9000 Ghent, Belgium
Email: ltessens@telin.ugent.be

A. Alecu and A. Munteanu
ETRO, Vrije Universiteit Brussel
Pleinlaan 2
B-1050 Brussels, Belgium

Abstract— In this paper, we perform an inter-sub-band statistical analysis of curvelet coefficients, making a distinction between two classes of coefficients: those representing useful image content and those dominated by noise. This analysis enables us to develop an appropriate inter-sub-band local spatial activity indicator (LSAI) for curvelets. We use this LSAI in our recently developed curvelet-based denoising method *ProbShrinkCurv*. The results demonstrate that the new method outperforms the wavelet-based *ProbShrink* estimator as well as the existing curvelet-based methods, both for textured and for piecewise smooth images.

I. INTRODUCTION

In recent years, many novel geometric image transforms have been developed, such as the ridgelet transform [1], the wedgelet transform [2] and the contourlet transform [3], just to name a few. These new transforms capture the geometric information present in images, and in this sense overcome the limitations of classical wavelets. Among these, a mathematically elegant method entitled the curvelet transform has gained increasing popularity [4]. Curvelets are directional basis functions that are highly localized, both in space and frequency. We refer the reader to [4] for a comprehensive description of the curvelet transform.

Joint image statistics in the curvelet domain were recently studied in [5]. In [6], we extended this analysis by focusing on the different behavior of curvelet coefficients representing significant image edges on the one hand, and coefficients dominated by noise on the other hand. Based on our findings and inspired by the wavelet domain *ProbShrink* estimator [7], we defined and analyzed different intra-band local spatial activity indicators (LSAIs) in the curvelet domain.

In this paper, we further extend the study of image statistics in the curvelet domain, now focusing on the correlation and dependency properties of curvelet coefficients in different sub-bands (again making a distinction between curvelet coefficients representing significant image edges and coefficients dominated by noise). This will allow us to design LSAIs that include inter-band correlated curvelet coefficients. We will use these LSAIs in the curvelet-based denoising method *ProbShrinkCurv* that we developed in [6].

The remainder of this paper is organized as follows: in Section II, some background information on the curvelet transform is provided and the notations and terminology used in this paper are introduced. In Section III, a comparative inter-band statistical analysis of the two classes of curvelet coefficients mentioned above is presented. Sections IV and V summarize the main results and conclusions of this paper.

II. THE CURVELET TRANSFORM

As in [6], we use the wrapping implementation of the digital curvelet transform [4], with a curvelet decomposition at the finest scale, throughout this paper. A motivation of this choice can be found in [6].

In Fig. 1, the curvelet decomposition of the test image *Barbara* is shown. The low-pass image is located in the center of the representation. The curvelet coefficients are displayed around it, grouped according to orientation and scale. The concentric coronae represent the different scales, starting with the lowest scale (low frequencies) in the center. Sub-bands of the same scale are ordered within these coronae so that the orientation suggested by their position matches the spatial frequencies they represent. For example, a horizontal line will produce high curvelet coefficients in the sub-bands that are located along a vertical line through the low-pass image. One can clearly discern four quadrants in each corona, which we will number in a clockwise direction, starting with the upper one. Quadrant 1 contains the real, quadrant 3 the imaginary parts of the (complex) curvelet coefficients produced by mostly horizontally (MH) oriented curvelet functions. Mutatis mutandis, the same holds for quadrant 2 and 4. So although the coefficients contained in the different quadrants are actually only the real or imaginary parts of the in reality complex curvelet coefficients, we will refer to these real and imaginary parts as ‘curvelet coefficients’. In Figure 1, curvelet coefficients with value zero are marked in gray, whereas large positive coefficients are bright and negative coefficients with a large absolute value are dark. From the prevalent gray color of Figure 1, it is clear that the curvelet decomposition of natural images is extremely sparse.

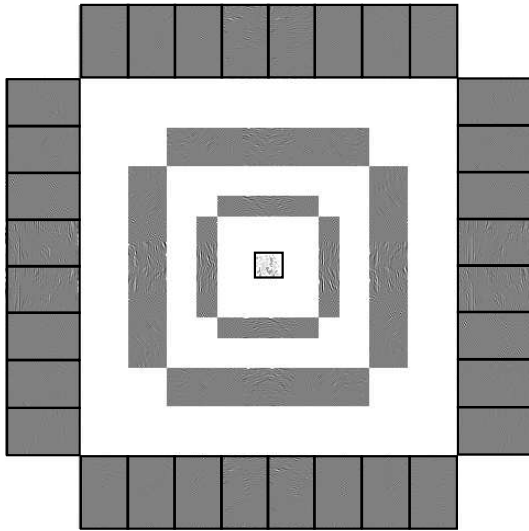


Fig. 1. The curvelet decomposition of 128×128 *Barbara*. The low-pass image is located at the center of the representation. The sub-bands of the finest scale are marked by black rectangles.

A. Terminology and Notations

In this paper we will use the same terminology as Alecu et al. [5]. Given a curvelet coefficient X , we will denote by

- N_i the neighboring curvelet coefficient in the same sub-band, where i denotes which one of the 8 neighbors is meant (all neighbors are numbered from 1 to 8, starting with the neighbor located at the upper left and proceeding clockwise).
- C_k the cousin curvelet coefficient located at the same relative position as X in a different sub-band at the same scale. k denotes which sub-band is meant (all sub-bands within each corona are numbered, starting with the sub-band at the upper left and proceeding clockwise).
 - C_k is an *adjacent* cousin of X if sub-band k lies next to the sub-band in which X is located.
 - C_k is an *opposing* cousin of X if sub-band k lies opposite the sub-band in which X is located, or in other words, if C_k is the real (imaginary) part of the complex curvelet coefficient of which X is the imaginary (real) part.
- P the parent curvelet coefficient, located at the same relative position as X in the same sub-band but at a coarser scale.

III. INTER-BAND CURVELET STATISTICS

In the study of Alecu et al. [5], it was found that curvelet coefficients of different sub-bands are approximately *de-correlated*, but some *dependencies* between sub-bands do exist. Alecu observed dependency between a curvelet coefficient and its parent, as well as between a curvelet coefficient and its cousins. The strength of these inter-orientation dependencies decreases with the increase of the difference in orientation, but one also observes dependency with respect to the opposite

orientation [5]. We will now further extend this study of inter-band curvelet statistics. As in [6], we will make a distinction between curvelet coefficients representing significant image edges and coefficients dominated by noise.

In practice, we will distinguish between these two classes of coefficients in the following way. We decompose a noise-free image into its curvelet coefficients. All coefficients with an absolute value greater than an empirically determined threshold T will be marked as significant, i.e. representing useful image content, the others will be marked as insignificant. This is justified because curvelets provide an optimally sparse representation of objects which display curve-punctuated smoothness - smoothness except for discontinuity along a general curve with bounded curvature [4]. Hence the curvelet representation of an image is close to the ideal case in which all coefficients representing image features are big, and all other coefficients are zero. Next, we decompose the same image into its curvelet coefficients, but this time the image is contaminated with white Gaussian noise with standard deviation σ . We now mark a curvelet coefficient as significant if the same curvelet coefficient was also significant in the noise-free curvelet decomposition, and similar for insignificant coefficients. The absolute value of the noise-free significant curvelet coefficients is big so we consider the influence of the noise on these coefficients to be negligible. The noise-free insignificant curvelet coefficients have an absolute value smaller than the threshold (most of them will be very close to zero), and we consider the noisy insignificant coefficients to be dominated by the noise.

All the histograms in this section have been obtained from the curvelet decomposition of a noise-contaminated version of *Barbara*. We remark that for other natural images, the obtained histograms are similar (and hence the corresponding correlation coefficients are of the same order of magnitude as the ones presented in this section). The standard deviation σ of the added Gaussian noise was 20 and the threshold between significant and insignificant coefficients was set to 1.4σ . For reasons of representation, all plots of conditional histograms have a logarithmic gray-scale.

A. Adjacent cousins

In Fig. 2a and 2b, the conditional histograms of the significant, respectively insignificant curvelet coefficients of a sub-band of the finest scale, conditioned on their adjacent cousins, are plotted. Both conditional histograms have an irregular shape, which indicates the dependency between both types of curvelet coefficients and their adjacent cousins. Furthermore, the conditional histograms appear to be slightly 'tilted'. This indicates some small correlation between the coefficients and their adjacent cousins. This observation is confirmed by the correlation coefficients calculated from this data (see Table Ia). The correlation is higher for the significant coefficients than for the insignificant ones (correlation coefficients of 0.1866 and 0.1178 respectively).

TABLE I

CORRELATION COEFFICIENTS BETWEEN SIGNIFICANT OR INSIGNIFICANT CURVELET COEFFICIENTS ON THE ONE HAND AND ON THE OTHER HAND (A) ADJACENT COUSINS, (B) OPPOSING COUSINS AND (C) PARENTS.

	Sign. coeffs.	Insign. coeffs.
a) Adjacent cousins	0.1994	0.1169
b) Opposing cousins	-0.0083	0.0139
c) Parents	-0.0051	0.0169

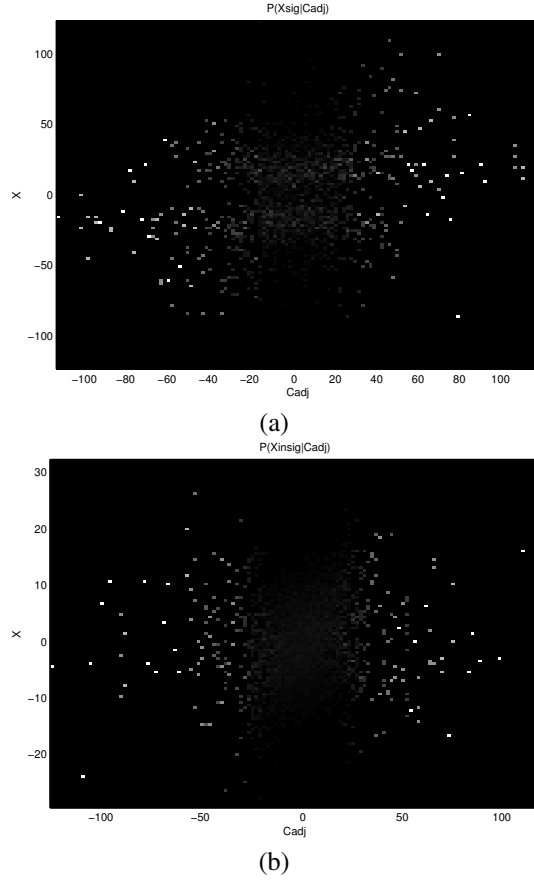


Fig. 2. Conditional histograms of the (a) significant and (b) insignificant curvelet coefficients, conditioned on their adjacent cousins.

B. Opposing cousins and parents

The conditional histograms of the significant and insignificant curvelet coefficients of a sub-band, conditioned on their opposing cousins, look very similar, except that one can no longer observe any correlation. Indeed, the correlation coefficients are very close to zero (see Table Ib). The same behavior (dependency but de-correlation) can be observed for curvelet coefficients conditioned on their parents (see Table Ic).

C. Local Spatial Activity Indicators

The LSAI of a curvelet coefficient is defined as a function of those coefficients that are well correlated when the coefficient represents a significant edge. In [6], we defined

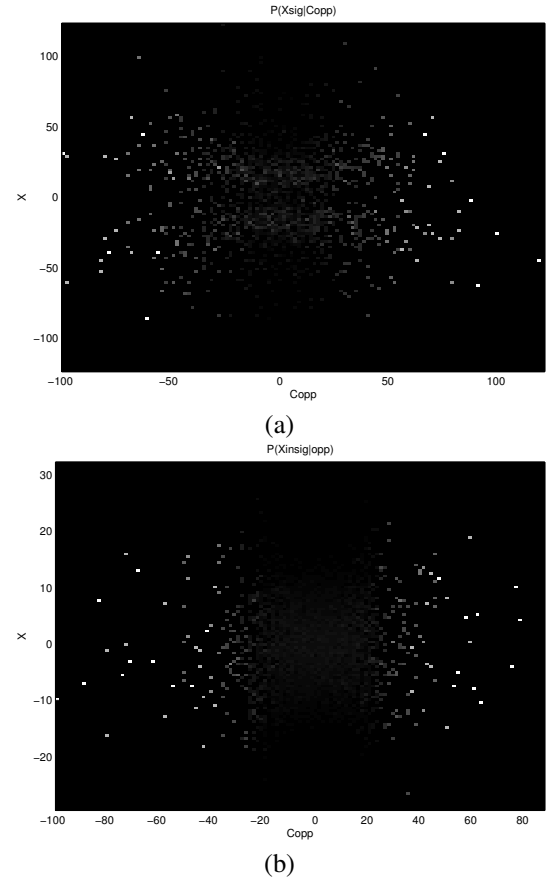


Fig. 3. Conditional histograms of the (a) significant and (b) insignificant curvelet coefficients, conditioned on their opposing cousins.

and analyzed different local spatial activity indicators (LSAIs) in the curvelet domain. All proposed LSAIs were calculated from intra-band coefficients. We will now evaluate 4 candidate LSAIs that are calculated from curvelet coefficients from other sub-bands:

- the *adjacent LSAI*: the mean absolute value of the two adjacent cousins of each coefficient.
- the *adjacent and opposing LSAI*: the mean absolute value of the two adjacent cousins and the opposing cousin of each coefficient.
- the *adjacent and parent LSAI*: the mean absolute value of the two adjacent cousins and the parent of each coefficient.
- the *adjacent, opposing and parents LSAI*: the mean absolute value of the two adjacent cousins and the opposing cousin of each coefficient, as well as its parent.

We will perform the evaluation in two ways: firstly by investigating the correlation between curvelet coefficients and their corresponding LSAIs, and secondly by plugging them into the curvelet-based denoising method we developed in [6]. The second evaluation will be performed in the next section.

1) *Adjacent Cousins LSAI*: In Fig. 4a and 4b, we have plotted the conditional histograms of the absolute value of the significant, respectively insignificant curvelet coefficients

TABLE II

CORRELATION COEFFICIENTS BETWEEN SIGNIFICANT OR INSIGNIFICANT CURVELET COEFFICIENTS ON THE ONE HAND AND ON THE OTHER HAND THE LSAI OF (A) ADJACENT COUSINS, (B) ADJACENT AND OPPOSING COUSINS, (C) ADJACENT COUSINS AND PARENTS AND (D) ADJACENT AND OPPOSING COUSINS AND PARENTS.

	Sign. coeffs.	Insign. coeffs.
a) adjacent LSAI	0.2699	0.0584
b) adjacent and opposing LSAI	0.3089	0.0798
c) adjacent and parents LSAI	0.3131	0.0670
d) adjacent, opposing and parents LSAI	0.3369	0.0576

of a sub-band of the finest scale, conditioned on the adjacent cousins LSAI. In Table IIa the correlation coefficients between the curvelet coefficients and this LSAI are indicated. From Fig. 4 and Table IIa, one can notice that the significant curvelet coefficients are more correlated with this LSAI than the insignificant coefficients. However, the correlation coefficient between them is not very high.

2) *Other Candidate LSAIs*: The conditional histograms of the absolute value of the significant, respectively insignificant curvelet coefficients of a sub-band of the finest scale, conditioned on the other candidate LSAIs look very similar to the conditional histograms of Figure 4. For this reason, we have not plotted them here. In Table IIb-d the correlation coefficients between the curvelet coefficients and these LSAIs are indicated. For all candidate LSAIs, similar conclusions as in Section III-C.1 can be drawn concerning the correlation properties of the significant and insignificant curvelet coefficients.

IV. DENOISING RESULTS

In Table III, the PSNR values of the denoising results of some 512x512 gray-scale images using the *ProbShrinkCurv* method of [6] are shown for the different LSAIs proposed in Section III-C, as well as for the best performing intra-band LSAIs of [6]. These best performing intra-band LSAIs are the intra-band isotropic LSAI, calculated as the mean absolute value of an isotropic region around each curvelet coefficient, and the intra-band anisotropic LSAI oriented in the direction of lowest correlation, calculated as the mean absolute value of an anisotropic region around each curvelet coefficient, oriented in the direction of lowest correlation.

From Table III we can see that among all inter-band LSAIs, using the adjacent, opposing and parent LSAI leads to the best denoising results. This agrees with our expectations, as the correlation coefficient between this LSAI and the significant curvelet coefficients is higher than for the other LSAIs (see Table II). The same holds for the difference in correlation coefficient between significant and insignificant coefficients. Table III also reveals that for piecewise smooth images such as *Lena* and *Peppers*, the inter-band LSAIs outperform the intra-band ones. For textured images such as *Barbara* and

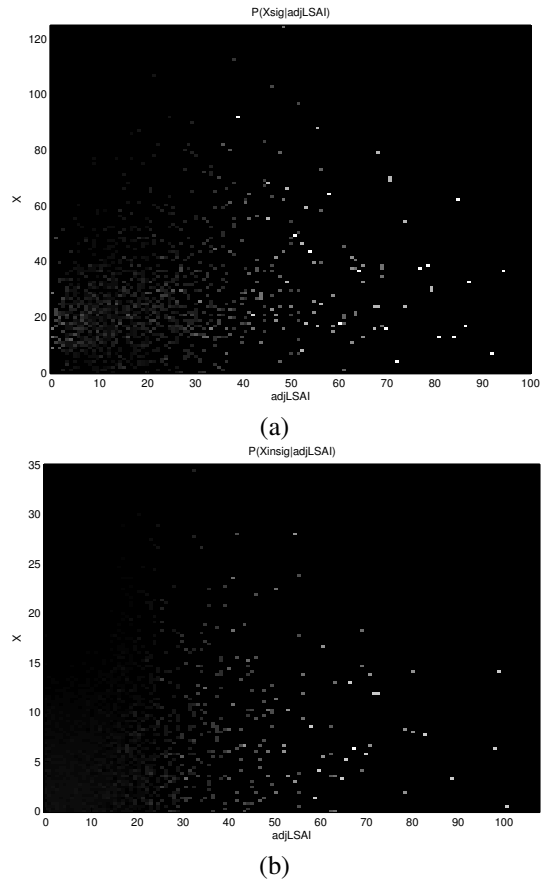


Fig. 4. Conditional histograms of the (a) significant and (b) insignificant curvelet coefficients, conditioned on the adjacent LSAI.

Baboon, both types of LSAIs are on a competitive basis. This is somewhat surprising, as the correlation between significant curvelet coefficients and the intra-band LSAIs is significantly higher than in the inter-band case. On the other hand, the correlation between insignificant curvelet coefficients and the inter-band LSAIs is also significantly lower than in the intra-band case, which might account for our observations.

In Fig. 5, we compare a detail of the denoising result on the 512x512 gray-scale *Barbara*-image of the *ProbShrinkCurv* method with the adjacent, opposing and parent LSAI with some state-of-the-art methods: the wavelet domain *ProbShrink* method [7], hard thresholding in the curvelet domain and the enhanced curvelet denoising method of Demanet that is included as a demo in the CurveLab Toolbox, Version 2.0 [8]. For this image, our results in terms of PSNR show improvement over the related wavelet-based technique [7] and over denoising by thresholding the curvelet coefficients [4]. The wavelet based method yields a PSNR of 29.50dB, hard thresholding the curvelet coefficients yields a PSNR of 29.02dB, and the new method yields a PSNR of 30.15dB. Hence, the improvement over hard-thresholding in the curvelet domain is 1.13dB and the improvement over the wavelet-based related method is smaller in terms of PSNR but visually significant. A similar visual improvement can be noticed over

TABLE III

ProbShrinkCurv DENOISING RESULTS OF SOME 512X512 GRAY-SCALE IMAGES, USING THE DIFFERENT LSAIS OF SECTION III-C. THE NOISY INPUT IMAGES ARE CONTAMINATED WITH WHITE GAUSSIAN NOISE WITH STANDARD DEVIATION 20. (A) DENOISING RESULTS USING THE ADJACENT LSAI, (B) THE ADJACENT AND OPPOSING LSAI, (C) THE ADJACENT AND PARENT LSAI, (D) THE ADJACENT, OPPOSING AND PARENT LSAI, (E) THE INTRA-BAND ISOTROPIC LSAI OF [6] AND (F) THE INTRA-BAND ANISOTROPIC LSAI ORIENTED IN THE DIRECTION OF LOWEST CORRELATION ([6]).

	Barbara	Lena	Peppers	Baboon
Input	22.16dB	22.14dB	22.22dB	22.12dB
a) Adjacent LSAI	30.07dB	32.16dB	31.27dB	26.54dB
b) Adjacent and opposing LSAI	30.11dB	32.29dB	31.33dB	26.48dB
c) Adjacent and parent LSAI	30.07dB	32.36dB	31.39dB	26.75dB
d) Adjacent, opposing and parent LSAI	30.15dB	32.50dB	31.48dB	26.71dB
e) Intra-band isotropic LSAI [6]	30.11dB	32.08dB	31.16dB	26.69dB
f) Intra-band anisotropic LSAI uncorrelated [6]	30.19dB	32.13dB	31.10dB	26.65dB

TABLE IV

DENOISING RESULTS OF SOME 512X512 GRAY-SCALE IMAGES. THE NOISY INPUT IMAGES ARE CONTAMINATED WITH WHITE GAUSSIAN NOISE WITH STANDARD DEVIATION 20. (A) DENOISING RESULTS OF *ProbShrinkCurv* USING THE ADJACENT, OPPOSING AND PARENT LSAI, (B) DENOISING RESULTS OF *ProbShrink* FOR WAVELETS, (E) DENOISING RESULTS OF HARD THRESHOLDING IN THE CURVELET DOMAIN, (F) DENOISING RESULTS OF THE ENHANCED CURVELET DENOISING METHOD OF DEMANET [8].

	Barbara	Lena	Peppers	Baboon
Input	22.16dB	22.14dB	22.22dB	22.12dB
a) ProbShrinkCurv	30.15dB	32.50dB	31.48dB	26.71dB
b) ProbShrinkWav	29.50dB	32.17dB	31.17dB	26.56dB
c) Curvelet HT	29.02dB	31.77dB	30.75dB	25.25dB
d) Curvelet Enhanced	30.07dB	32.29dB	31.27dB	26.22dB

the method of Demanet [8] (less artifacts, see Fig. 5), although the result of this technique is comparable in terms of PSNR.

In Table IV, we compare the performance in terms of PSNR of the same methods for some other gray-scale images. We notice that for both textured and piecewise smooth images, the *ProbShrinkCurv* method using the inter-band adjacent, opposing and parent LSAI outperforms all other methods.

V. CONCLUSION

In this paper, we investigated the differences in inter-sub-band statistical dependencies and correlations between curvelet coefficients representing significant images features and those dominated by noise.

We used this difference in behavior to design different inter-sub-band local spatial activity indicators for the *ProbShrink* estimator from [7], adapted to curvelets. We showed that especially for piecewise smooth images, using an inter-sub-band local spatial activity indicator instead of an intra-sub-band one is beneficial. The resulting denoising method outperforms its wavelet-based counterpart and other curvelet-based methods in terms of PSNR and visually, both for textured as for piecewise smooth images.

In future work, we will investigate combinations of intra-band and inter-band LSAIs.

ACKNOWLEDGMENT

The author L. Tessens is supported as a Research Assistant by the Research Foundation - Flanders (FWO - Flanders). A. Pižurica is a postdoctoral research fellow of FWO Flanders.

REFERENCES

- [1] E. J. Candes and D. L. Donoho, "Ridgelets: a key to higher-dimensional intermittency," *Phil. Trans. R. Soc. London A.*, pp. 2495–2509, 1999.
- [2] D. Donoho, "Wedgelets: nearly minimax estimation of edges," *The Annals of Statistics*, pp. 859–897, 1999.
- [3] M. N. Do and M. Vetterli, "The contourlet transform: An efficient directional multiresolution image representation," *IEEE Transactions on Image Processing*, vol. 14, no. 12, pp. 2091 – 2106, 2005. [Online]. Available: <http://dx.doi.org/10.1109/TIP.2005.859376>
- [4] E. J. Candes, L. Demanet, D. L. Donoho, and L. Ying, "Fast discrete curvelet transforms," Applied and Computational Mathematics, Caltech, Tech. Rep., 2005.
- [5] A. Alecu, A. Munteanu, A. Pizurica, W. Philips, J. Cornelis, and P. Schelkens, "Information-theoretic analysis of dependencies between curvelet coefficients," in *Proceedings of the ICIP*, 2006.
- [6] L. Tessens, A. Pižurica, A. Alecu, A. Munteanu, and W. Philips, "Spatially adaptive image denoising based on joint image statistics in the curvelet domain," in *Proceedings of SPIE - The International Society for Optical Engineering*, Boston, Oct. 2006, to appear.
- [7] A. Pizurica and W. Philips, "Estimating the probability of the presence of a signal of interest in multiresolution single- and multiband image denoising," *IEEE Transactions on Image Processing*, vol. 15, no. 3, pp. 654 – 665, 2006. [Online]. Available: <http://dx.doi.org/10.1109/TIP.2005.863698>
- [8] E. J. Candes, L. Demanet, D. L. Donoho, and L. Ying, "Curvelet toolbox, version 2.0," <http://www.curvelet.org>, 2005. [Online]. Available: <http://www.curvelet.org>

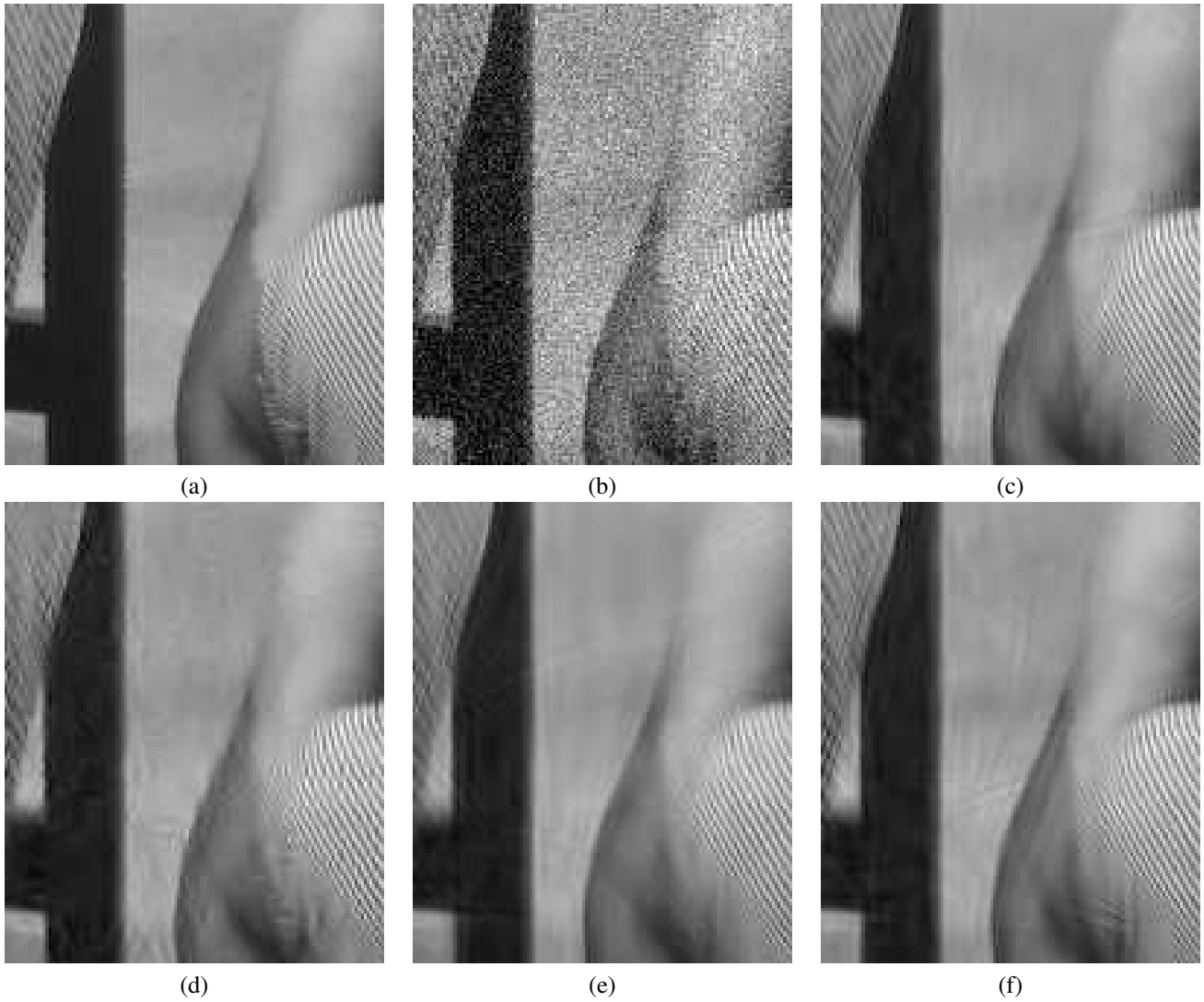


Fig. 5. Detail of the denoising results of *Barbara*. (a) the original image, (b) the noisy image (noise standard deviation 20, PSNR=22.16dB), (c) *ProbShrinkCurv* denoising result using the adjacent, opposing and parent LSAI (PSNR=30.15dB), (d) denoising result of *ProbShrink* for wavelets (PSNR=29.50dB), (e) denoising result of hard thresholding in the curvelet domain (PSNR=29.02dB), (f) denoising result of the enhanced curvelet denoising method of Demanet[8] (PSNR=30.13dB).